ELSEVIER

Coordination Chemistry Reviews
148 (1996) 199–219

COORDINATION CHEMISTRY REVIEWS

Preparation of chiral and *meso*-crown ethers incorporating cyclohexane-1,2-diol derivatives as a steric barrier and their complexation with chiral and achiral amines

Koichiro Naemura [a], Yoshito Tobe [a], Takahiro Kaneda [b]

[a] *Department of Chemistry, Faculty of Engineering Science, Osaka University, Toyonaka, Osaka 560, Japan*
[b] *The Institute of Science and Industrial Research, Osaka University, Mihogaoka, Ibaraki, Osaka 567, Japan*

Received 2 February 1995; revised 15 June 1995

Contents

Abstract

The design and synthesis of chiral crown ethers possessing a chiral recognition ability which carry great potential for separation of enantiomers and analytical purpose has become an important and rapidly growing field of host–guest chemistry. One of the advantages of crown ethers constructed using a synthetic chiral building block is that it is rather easy to modify the chiral cavity resulting in the improvement in enantiomer selectivity. Cyclohexane-1,2-diol derivatives such as *cis*-1-phenylcyclohexane-1,2-diol, *trans*-1-phenylcyclohexane-1,2-diol and *trans*-1,2-diphenylcyclohexane-1,2-diol are of interest as chiral building blocks of crown ethers, because incorporation of these subunits into the 18-crown-6 framework causes a reduction in conformational flexibility of the chiral cavity and fixes the phenyl chiral barrier perpendicularly above the face of crown ring to modify enantiomer recognition ability.

Chiral crown ethers of the 18-crown-6 type were synthesized using these building blocks and their chiral recognition behaviour in differential enantiomer transport through bulk

0010-8545/96/$32.00 © 1996 Elsevier Science S.A. All rights reserved
SSDI 0010-8545(95)01189-7

liquid membranes were examined. Chiral azophenolic crown ethers containing *cis*-1-phenylcyclohexane-1,2-diol or *cis*-cyclohexane-1,2-diol which can bind neutral amines to form a stable complex and exhibit enantiorecognitive coloration in complexation with chiral amines were prepared and the association constants for their complexes with chiral ethylamine and ethanolamine derivatives were determined on the basis of UV–visible absorbance.

The observed enantioselectivity is rationalized in terms of complementarity between a host and a guest as indicated by CPK molecular model examination. The alternation of the position of chiral barriers resulted in a reversal of the enantioselectivity.

Crown ethers with diastereotopic faces can bind a guest to each side of the diastereotopic faces to form diastereoisomeric complexes which occasionally cause troublesome "sidedness" problems. In order to avoid the problems, most crown ethers previously prepared contained at least one C_2 axis of symmetry. However, diastereotopic face selectivity in complexation does provide helpful information on the complexing behaviour of crown ethers to assist in the design of more elaborate and structured host molecules.

meso-Crown ethers having *cis*-1-phenylcyclohexane-1,2-diol were prepared and the diastereotopic face selectivity by their diastereotopic faces in complexation with achiral amines was examined by temperature-dependent ^1H nuclear magnetic resonance. Ethanolamine is attached stereoselectively to one of the faces to give one of diastereoisomeric complexes and the alternation of the position of steric barriers led to reversal of the diastereotopic face selectivity. A prediction of which diastereoisomeric complex is formed is made on the basis of CPK molecular model.

Keywords: Chiral crown ether; Chiral azophenolic crown ether; *meso*-Crown ether; Enantioselectivity in complexation; Diastereotopic face selectivity in complexation

1. Introduction

In 1967, Pedersen's papers on a crown ether described the synthesis of 33 crown ethers and their complexation with metal cations and ammonium salts [1]. Many chemists have been attracted by the characteristic complexation behaviour of crown ethers with guest species and a large number of papers on the design, preparation and complexation of crown ethers have been published [2]. Since Cram and his coworkers prepared optically active crown ethers having binaphthyl chiral subunits which exhibited high enantiomer-selective complexation with chiral organic ammonium salts and amino acid salts [3], the design and synthesis of enantioselective crown ethers which carry great potential for separation of enantiomers and analytical purpose has become an important and rapidly growing field of host–guest chemistry.

We have also been interested in the chiral recognition behaviour of crown ethers toward chiral amines and organic ammonium salts and synthesized various kinds of optically active crown ethers using synthetic subunits [4]. Recently, our continuing interest in this field prompted us to examine the enantiomer recognition behaviour of chiral crown ethers incorporating cyclohexane-1,2-diol derivatives as a chiral subunit. As can be seen in Figs. 1 and 2, the structural features of these crown ethers are that the cyclohexane moiety incorporated with an 18-crown-6 framework reduces conformational flexibility of the chiral cavity of the crown ether compared with that of crown ethers containing an open chain subunit such as 1-phenylethane-1,2-diol and the bulky phenyl barrier extends perpendicularly above the face of crown ring

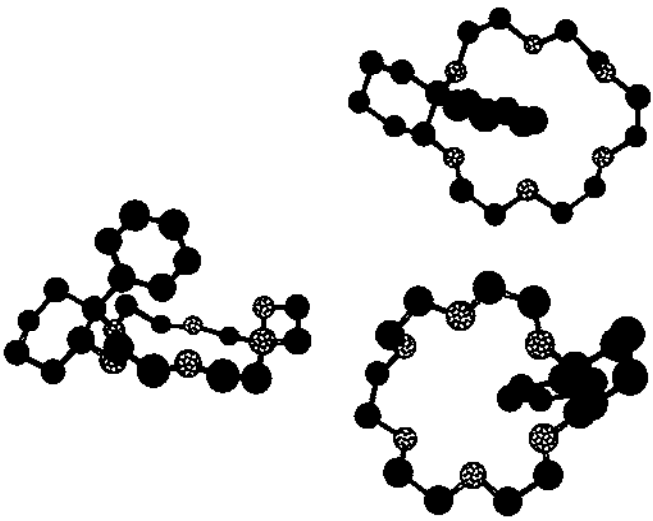

(*R,R*)-1

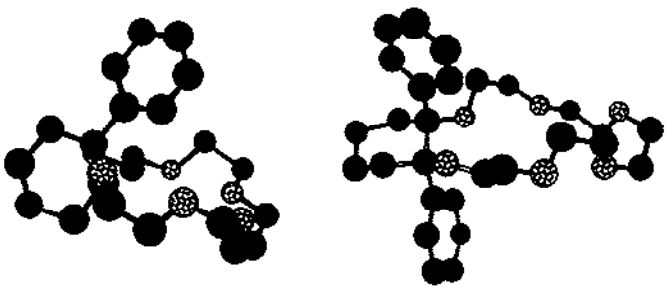

(*R,S*)-3 (*R,R*)-5

Fig. 1. Structures of the calculated conformers of (*R,R*)-1, (*R,S*)-3 and (*R,R*)-5.

to serve as an efficient chiral barrier. Conformational inflexibility of the chiral cavity and the chiral barrier is generally expected to improve the enantiomer recognition ability of chiral crown ethers.

The first of the following sections describes the enantiomer recognition behaviour of crown ethers **1**, **2**, **3** and **5** of the type 18-crown-6 incorporating *cis*-1-phenylcyclohexane-1,2-diol (**6**), *trans*-1-phenylcyclohexane-1,2-diol (**7**) and *trans*-1,2-diphenylcyclohexane-1,2-diol (**8**) as chiral subunits [5]. Their enantiomer selectivities are interpreted in terms of the complementarity between a host and a guest on the basis of CPK molecular models.

The binding ability of crown ethers is characteristically influenced by replacing one or more ether oxygen atoms by another heteroatom or group capable of electron

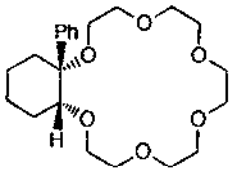

(*R,R*)-(-)-**1**

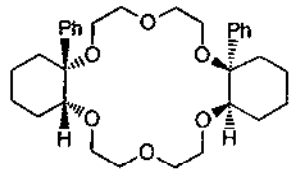

(*R,R*)(*R,R*)-(-)-**2**

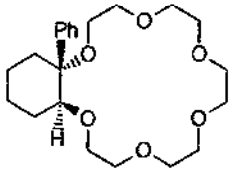

(*R,S*)-(+)-**3**

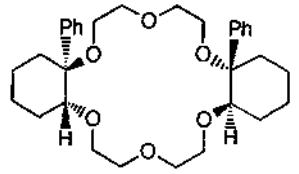

(*S,R*)(*S,R*)-**4**

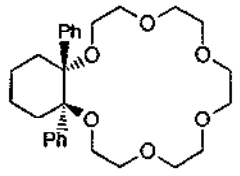

(*R,R*)-(-)-**5**

donating. In view of this, azophenolic crown ethers having the phenolate oxygen atom as a binding site are of interest because they can bind neutral amines to form a stable complex and exhibit enantiorecognitive coloration in complexation with chiral amines [6]. Examination of enantiorecognitive coloration is the first step toward developing colour indicators to judge the absolute configuration of chiral amines on the basis of host–guest complexation.

In the third section, the enantiomer recognition behaviour of optically active azophenolic crown ethers **23** and **24** [7] incorporating the chiral subunit **6** is described and their enantiomer selectivities analysed by their association constants are discussed in terms of host–guest complementarity. The enantiomer selectivity of the azophenolic crown ether **28** [8] containing the *cis*-cyclohexane-1,2-diol residues is discussed in the fourth section.

Crown ethers with diastereotopic faces can bind a guest to each side of the face of a crown ring to form diastereoisomeric α and β complexes. The "sidedness" problems in complexation are somewhat troublesome in the diastereoisomeric complexation of chiral crown ethers **1** and **3** with a chiral ammonium salt. In order to avoid "sidedness" problems, most of the chiral and achiral crown ethers previously

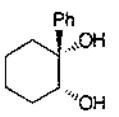

(1*R*,2*R*)-(+)-**6**

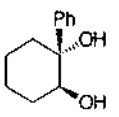

(1*R*,2*S*)-(+)-**7**

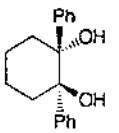

(1*R*,2*R*)-(-)-**8**

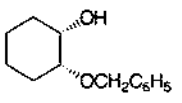

(1*S*,2*R*)-(-)-**9**

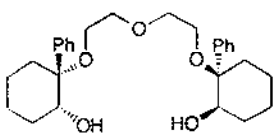

(-)-**10**

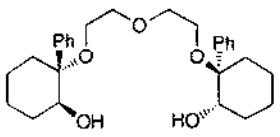

(+)-**11**

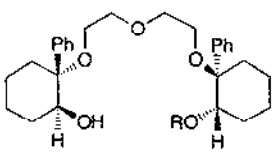

R = $(CH_2)_2O(CH_2)_2OMs$

(+)-**12**

prepared contain at least one C_2 axis of symmetry, so the same complexes are formed by attachment of a guest to either side of the crown ring. However, the diastereotopic face selectivity in complexation of a crown ether is of interest; examination of the selectivity would provide helpful information on the complexing behaviour of crown ethers to assist in the design of more elaborate and structured hosts.

We have prepared crown ethers **55** and **56** of a *meso* type containing **6** as a steric barrier, the plane of symmetry of which is perpendicular to the plane defined by the polyether ring, to make the faces diastereotopic [9]. In the last section, we describe the diastereotopic face selectivity of **55** and **56** in complexing achiral amines and we discuss which diastereoisomeric complex of *meso*-crown ethers with ethanolamine was selectively formed.

2. Enantiomer recognition of optically active crown ethers 1, 2, 3 and 5 of the type 18-crown-6 incorporating *cis*-1-phenylcyclohexane-1,2-diol, *trans*-1-phenylcyclohexane-1,2-diol and *trans*-1,2-diphenylcyclohexane-1,2-diol as chiral subunits

The use of enzymes as chiral catalysts for the synthesis of chiral synthons has been well documented recently [10] and, in particular, hydrolases such as lipases

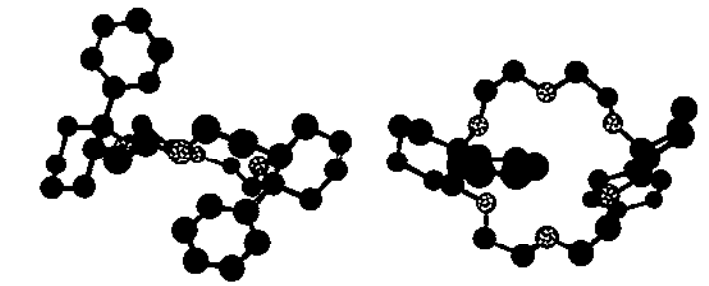

(*R,R*)(*R,R*)-**2**

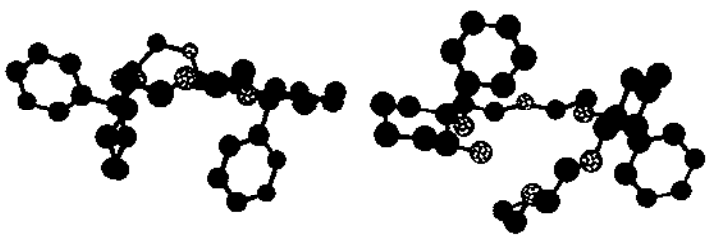

(*S,R*)(*S,R*)-**4** (*S,R*)(*S,R*)-**12**

Fig. 2. Structures of the calculated conformers of (*R,R*)(*R,R*)-**2**, (*S,R*)(*S,R*)-**4**, (*S,R*)(*S,R*)-**12**.

and esterases are attractive for the preparation of an optically active diol, that is, a chiral subunit. Optically active subunits (1*R*,2*R*)-(+)-**6** and (1*S*,2*R*)-(−)-**7** were prepared by the pig liver esterase catalysed hydrolysis of (±)-*cis*-2-acetoxy-1-phenylcyclohexanol and (±)-*trans*-2-acetoxy-1-phenylcyclohexanol respectively. The third chiral subunit (1*R*,2*R*)-(−)-**8** was prepared from (1*R*,2*R*)-(+)-**6**.

Recently, hydrolase-catalysed transesterification in organic solvents [11] has been noted as a convenient method for the optical resolution of alcohols. (1*S*,2*R*)-(−)-*cis*-2-benzyloxycyclohexanol (**9**) which is the chiral subunit of **28** was resolved by the lipase-catalysed enantiomer selective acylation of (±)-**9**.

First the chiral crown ethers (*R,R*)-(−)-**1** (62% yield), (*S,R*)-(−)-**3** (25% yield) and (*R,R*)-(−)-**5** (15% yield) were prepared from (1*R*,2*R*)-(+)-**6**, (1*S*,2*R*)-(−)-**7** and (1*R*,2*R*)-(−)-**8** respectively. The relatively low yields of (*S,R*)-(−)-**3** and (*R,R*)-(−)-**5** are attributed to their high steric energy (the MM2 steric energy: **3**, 54.3 kcal mol^{-1}; **5**, 58.2 kcal mol^{-1}) compared with that of **1** (44.5 kcal mol^{-1}).

In the stepwise syntheses of the crown ethers **2** and **4** possessing two subunits of the same chirality and one C_2 axis of symmetry lying in the plane of the crown ring, the *cis*-anti-*cis* diol **10** and the *trans*-anti-*trans* diol **11** were required as the key intermediates of C_2 symmetry.

The high dilution condensation of (*R,R*)(*R,R*)-(−)-**10** with diethylene glycol bis(toluene-*p*-sulphonate) gave (*R,R*)(*R,R*)-(−)-**2** in moderate yield. The notation

(*R,R*)(*R,R*)-(−)-**2** in this review means that (−)-**2** contains two chiral subunits of the same (*R,R*) configuration. However, the same reaction of (*S,R*)(*S,R*)-(+)-**11** gave (*S,R*)(*S,R*)-(+)-**12** as a sole product and any cyclized products were not detected. The MM2 steric energy difference between **2** (51.4 kcal mol^{-1}) and **4** (61.9 kcal mol^{-1}) is ca. 10 kcal mol^{-1} and we suppose that the high steric energy of the latter is the reason for our unsuccessful preparation of **4**.

Enantiomer-selective complexations of (*R,R*)-(−)-**1**, (*R,R*)(*R,R*)-(−)-**2**, (*S,R*)-(−)-**3** and (*R,R*)-(−)-**5** with methyl (±)-phenylglycinate hydrochloride were evaluated by differential enantiomer transport through bulk liquid membranes containing the crown ether [12] demonstrating that (*R,R*)-(−)-**1**, (*R,R*)(*R,R*)-(−)-**2**, (*S,R*)-(−)-**3** and (*R,R*)-(−)-**5** formed the complex preferentially with the (*S*)-guest in respectively 3%, 16%, 8% and 14% enantiomeric excess.

The observed enantiomer selectivities are interpreted in terms of complementarity between the crown ether and the guest on the basis of the geometries **13–17** which are predicted from the well-known three-point binding mode and are based on the calculated conformations of **1**, **2** and **5** (Figs. 1 and 2) together with CPK molecular models of the complexes.

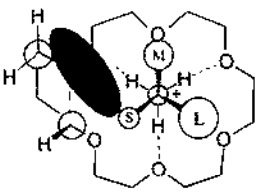

[(*R,R*)-**1**; chiral ammonium salt]

13

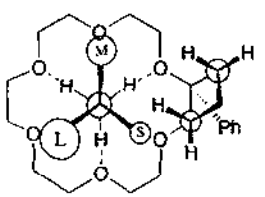

14

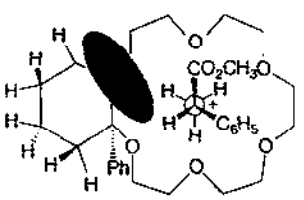

15 [(*R,R*)-**5**:(*S*)-guest]

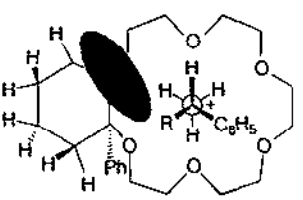

R=CO_2CH_3

16 [(*R,R*)-**5**:(*R*)-guest]

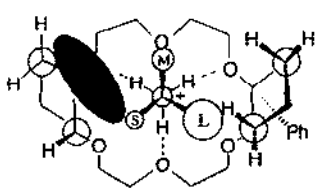

[(*R,R*)(*R,R*)-**2**; chiral ammonium salt]

17

In complexation of (*R,R*)-**1** and (*S,R*)-**3** possessing no C_2 axis of symmetry, the guest can be attached to each side of the diastereotopic faces of the crown ring to form the diastereoisomeric α and β complexes. We assume that the prerequisites for the favourable geometry of the complex are (1) the site near the bulky phenyl barrier is the most hindered area and so the S group should be placed here, (2) the M group occupies the somewhat hindered area over the diethylene glycol bridge because of the steric repulsion between the phenyl barrier and the guest, and (3) the L group is placed at the least hindered area. The geometry **13** is illustrated for the favourable β complex of (*R,R*)-**1** with a chiral ammonium salt of the type $LMSC^*NH_3^+$ (L, M and S are large, medium and small groups respectively). Therefore, when the guest is attached to the β face, the (*R,R*)-**1**–(*S*)-guest complex is more favourable than the (*R,R*)-**1**–(*R*)-guest complex because of the bulk ordering $C_6H_5 > CO_2CH_3 > H$. On the contrary, the favourable conformation of the α complex is illustrated in the geometry **14** where the S group is placed at the most hindered site near the cyclohexane barrier and the L group occupies the less hindered area suggesting that the direction of the chiral bias is opposite to that of **13**. The observed low enantiomer selectivity of (*R,R*)-**1** is assumed to be due to the "sidedness" problems, that is, the combination (*R,R*)-**1**–guest led to the α and β complexes compensating the enantiomer selectivity of this crown ether with each other.

The crown ethers (*R,R*)(*R,R*)-**2** and (*R,R*)-**5** of C_2 symmetry exhibited well-defined enantiomer selectivity. The proposed conformations of the complexes (*R,R*)-**5**–(*S*)-guest and (*R,R*)-**5**–(*R*)-guest are shown in the geometries **15** and **16** respectively. The observed enantiomer selectivity is interpreted in terms of the complementarity between (*R,R*)-**5** and (*S*)-guest, and the lack of complementarity in the (*R,R*)-**5**–(*R*)-guest complex.

The geometry **17** is illustrated for the favourable (*R,R*)(*R,R*)-**2**–chiral guest complex. It is easily understandable from **17** ($L=C_6H_5$, $M=CO_2CH_3$, $S=H$) that the combination (*R,R*)(*R,R*)-**2**–(*S*)-guest led to the stable complex.

The observations that (1) *cis*-1-phenylcyclohexane-1,2-diol was useful as a chiral subunit and (2) (*R,R*)(*R,R*)-(−)-**2** possessing the same subunit as (*R,R*)-**1** exhibited relatively high enantiomer selectively suggest that C_2 crown ethers possessing homotopic faces is favourable for selecting enantiomers of a guest.

3. Enantiomer recognition of the azophenolic crown ethers 23 and 24 incorporating a *cis*-1-phenylcyclohexane-1,2-diol subunit

As accepted from previous work [6,13], the phenolate oxygen atom necessarily participates in hydrogen bonding between a crown ether and an amine, and hence a three-point binding structure is unambiguously illustrated as shown in geometry **18** for the azophenolic crown ether–amine complex.

The phenol moiety is substituted for one of the CH_2OCH_2 groups of (*R,R*)(*R,R*)-**2** to give the phenolic crown ethers (*R,R*)(*R,R*)-**19** and (*R,R*)(*R,R*)-**20** which possess a similarly shaped cavity but a different placement of the phenol moiety with respect

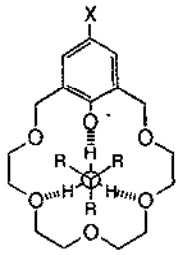

18

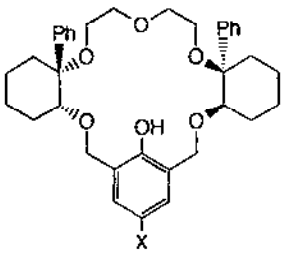

(*R,R*)(*R,R*)-**19**

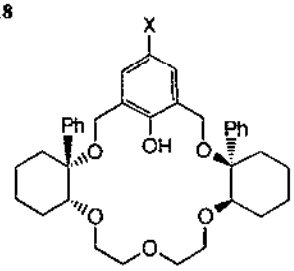

(*R,R*)(*R,R*)-**20**

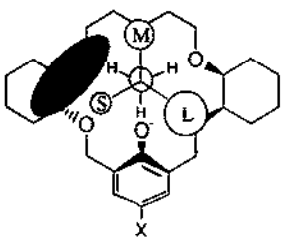

21

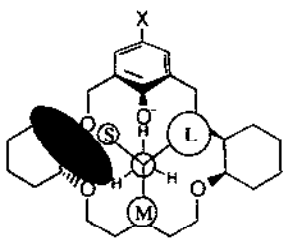

22

to the phenyl barriers. As indicated by spectroscopic evidence mentioned in a later section, the phenol moiety in a complex tilts out of the plane defined by the ether oxygen atoms and rather restricts the conformational mobility of the phenyl barriers resulting in improvement in the enantiomer selectivity of these crown ethers. With the assumptions described above and host–guest complementarity, the general geometry **21** is illustrated for the favourable complex of (*R,R*)(*R,R*)-**19** with a chiral amine and an anticlockwise LMSC*NH_2 sequence of groups (L→M→S). Similarly, the favourable combination (*R,R*)(*R,R*)-**20**–chiral amine leads to a complex with the general geometry **22** and a clockwise sequence of groups. Thus alteration of the position of the phenolate binding site causes configurational biases that are opposite to one another, and so the enantiomer selectivities of the azophenolic crown ethers **23** and **24** are expected to be the reverse of one another.

Through *para* substitution of the phenol moiety it is possible to make controlled

changes in the binding ability of the phenolic crown ether without altering the constitution of the crown ring [13]. The *para* substitution of an electron-withdrawing group such as the 2,4-dinitrophenylazo group is expected to enhance the acidity of phenolate oxygen resulting in enhancement of the stability of complex of the phenolic crown ether with an amine.

The azophenolic crown ethers (*R*,*R*)(*R*,*R*)-**23** and (*R*,*R*)(*R*,*R*)-**24** were prepared from (1*R*,2*R*)-(+)-**6**. The intermediate crown ethers (*R*,*R*)(*R*,*R*)-(−)-**25** and (*R*,*R*)(*R*,*R*)-(+)-**26** exhibited chiral recognition behaviour toward racemic organic ammonium salts such as ethyl (±)-phenylalaninate hydrochloride.

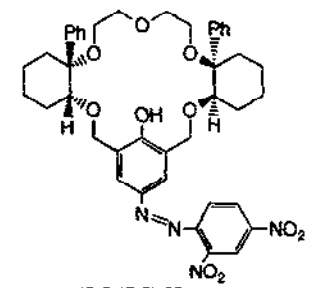

(*R*,*R*)(*R*,*R*)-**23**

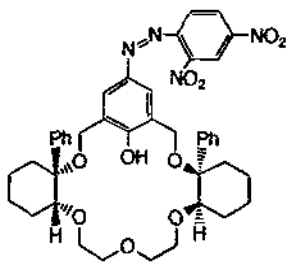

(*R*,*R*)(*R*,*R*)-**24**

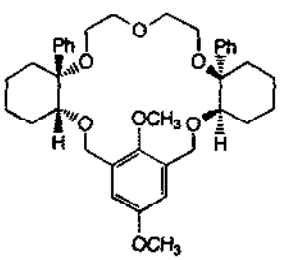

(-)-**25**

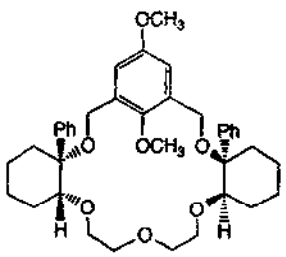

(+)-**26**

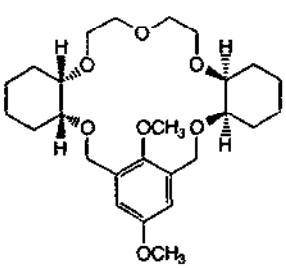

(-)-**27**

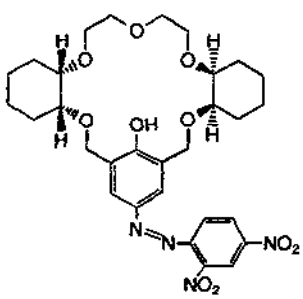

(*R*,*S*)(*R*,*S*)-**28**

Crown ethers incorporating the 2,4-dinitrophenylazophenol group exhibit a red shift in the UV–visible spectrum on formation of a complex with amines. The association constant for complexes of azophenolic crown ethers with amines was determined by the Benesi–Hildebrand method [14] on the basis of the absorbance

of a UV–visible spectrum (350–700 nm) in a non-polar medium: $CHCl_3$ at 25 °C. The observed association constants K_a and absorption maxima λ_{max} for chiral crown ether complexes with chiral amines are summarized in Table 1; those for the complexes with achiral amines are given in Table 2.

The observation that the K_a values for complexes of **23** and **24** with **36** are smaller than those for complexes with **35** is rationalized in terms of the reduced basisity of **36** compared with that of **35**. It is significant regarding the structure of the complex that, in spite of the reduced basisity of **37**, complexes with **37** had rather large K_a values. The facts suggested that a fourth hydrogen bond between the phenolate oxygen and the hydroxyl group of the guest stabilizes these complexes further. The weak binding ability toward **38** is due to the one-point binding mode in the corresponding complexes. Differences in λ_{max} values between diastereoisomeric sets of complexes, that is, enantiorecognitive coloration, were observed for the azophenolic

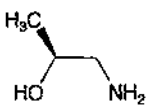

(*S*)-**29**

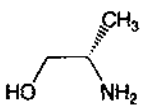

(*S*)-**30**

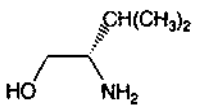

(*S*)-**31**

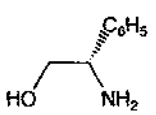

(*S*)-**32**

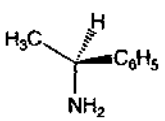

(*S*)-**33**

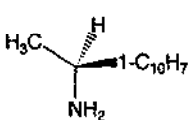

(*S*)-**34**

$CH_3CH_2CH_2NH_2$

35

$CH_3OCH_2CH_2NH_2$

36

$HOCH_2CH_2NH_2$

37

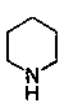

38

crown ether and the chiral amine combinations, e.g. $\lambda_{max} = 577$ nm and $\lambda_{max} = 583$ nm for the more stable (*S,S*)(*S,S*)-**23**–(*S*)-**29** complex and the less stable (*R,R*)(*R,R*)-**23**–(*S*)-**29** complex respectively. These observations provide basic information for the development of colour indicators to determine the absolute configuration of chiral amines.

Next, the enantiomer selectivity, that is, relative ratio of K_a values for the diastereoisomeric sets of complexes, is rationalized in terms of the host–guest complementarity which is examined using CPK molecular models of the complexes. These models

show that the general geometries **39** and **40** are visualized for the complexes (*R,R*)(*R,R*)-**23**–chiral amine and (*S,S*)(*S,S*)-**23**–chiral amine respectively. On the basis of the bulk ordering aryl > CH_3 > H it is understandable from these geometries that (*S*)-**33** and (*S*)-**34** exhibit better complementarity to (*S,S*)(*S,S*)-**23** than to (*R,R*)(*R,R*)-**23**.

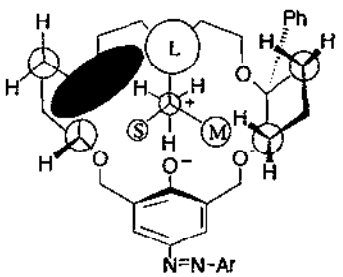

39 [(*R,R*)(*R,R*)-**23**: chiral amine]

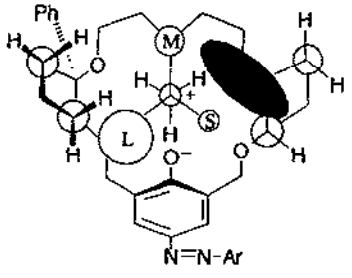

40 [(*S,S*)(*S,S*)-**23**: chiral amine]

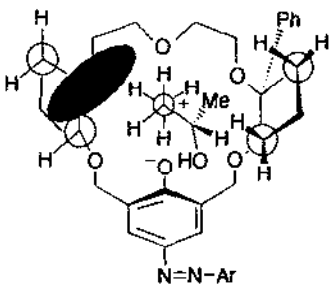

41 [(*R,R*)(*R,R*)-**23**:(*S*)-**29**]

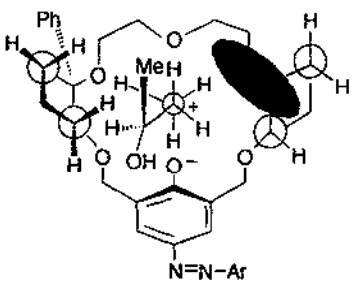

42 [(*S,S*)(*S,S*)-**23**:(*S*)-**29**]

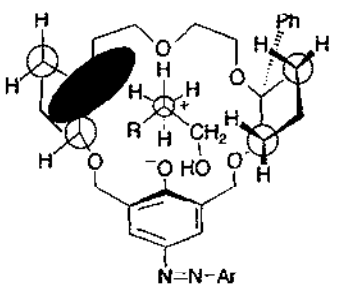

43 [(*R,R*)(*R,R*)-**23**:(*S*)-amine]

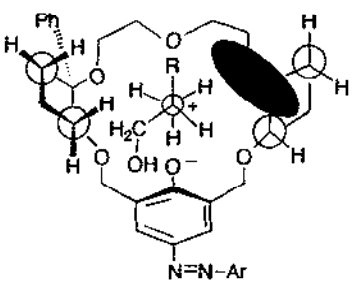

44 [(*S,S*)(*S,S*)-**23**:(*S*)-amine]

The relatively large K_a values for complexes of **23** with the ethanolamine derivatives (*S*)-**29** and (*S*)-**30** suggest that the complexes were stabilized by the fourth hydrogen bond. Thus, on the assumption that the hydroxymethyl group of the amines preferentially occupies the less hindered cyclohexane side, near the phenolate oxygen, making the fourth hydrogen bond, the geometries **41**–**44** are illustrated for complexes of **23** with chiral ethanolamine derivatives. This rationalizes the fact that the combinations (*S,S*)(*S,S*)-**23**–(*S*)-ethanolamines exhibited a larger K_a value than the diastereoisomeric combinations. The combination (*S,S*)(*S,S*)-**23**–(*S*)-**29** led to the more stable

Table 1
Association constants K_a (M^{-1}), absorption maxima λ_{max} and the ratio of K_a values for the complexes of chiral crown ethers with chiral amine

Host	Amine (*S*)	K_a values (M^{-1})		λ_{max} (nm)		(*R*,*R*,*R*,*R*):(*S*,*S*,*S*,*S*) K_a ratio
		(*R*,*R*,*R*,*R*)-host		(*S*,*S*,*S*,*S*)-host		
23	None	418				
23	**29**	197±1	(583)	270±2	(577)	0.730
23	**30**	78.4±2.3	(577)	88.3±0.6	(578)	0.888
23	**31**	18.6±0.3	(574)	19.3±0.2	(574)	0.964
23	**33**	5.3±0.3	(588)	11.1±0.4	(585)	0.477
23	**34**	4.3±0.2	(586)	8.3±0.3	(584)	0.518
24	None	418				
24	**29**	583±7	(589)	499±4	(588)	1.17
24	**30**	126±2	(583)	90.0±1.5	(585)	1.40
24	**31**	9.79±0.3	(579)	11.3±0.2	(580)	0.866
24	**33**	18.8±0.7	(599)	9.97±0.43	(597)	1.89
24	**34**	7.81±0.31	(595)	5.66±0.15	(598)	1.38
28	None	408				
28	**29**	182±2	(569)	184±2	(567)	0.989
28	**30**	151±2	(562)	92.9±1	(558)	1.63
28	**31**	38.5±0.2	(572)	26.1±0.7	(572)	1.48
28	**32**	33.2±0.7	(557)	10.9±1.0	(558)	3.02
28	**33**	14.8±0.5	(566)	23.9±0.3	(558)	0.619
28	**34**	9.2±0.1	(564)	15.0±0.5	(560)	0.613

Table 2
Association constants K_a (M^{-1}) and absorption maxima λ_{max} for the complexes of chiral and *meso*-crown ethers with achiral amine

Host	Amine	K_a values (M^{-1})	λ_{max} (nm)
(*R*,*R*)(*R*,*R*)-**23**	**35**	2.56×10^2	598
(*R*,*R*)(*R*,*R*)-**23**	**36**	5.94×10	600
(*R*,*R*)(*R*,*R*)-**23**	**37**	4.13×10^2	579
(*R*,*R*)(*R*,*R*)-**23**	**38**	1.31×10	592
(*R*,*R*)(*R*,*R*)-**24**	**35**	1.79×10^3	598
(*R*,*R*)(*R*,*R*)-**24**	**36**	3.47×10^2	599
(*R*,*R*)(*R*,*R*)-**24**	**37**	9.53×10^2	588
(*R*,*R*)(*R*,*R*)-**24**	**38**	7.11	598
(*R*,*S*)(*R*,*S*)-**28**	**35**	4.20×10^2	588
(*R*,*S*)(*R*,*S*)-**28**	**36**	6.71×10	588
(*R*,*S*)(*R*,*S*)-**28**	**37**	3.28×10^2	567
(*R*,*S*)(*R*,*S*)-**28**	**38**	3.90×10	576
meso-**55**	None		414
meso-**55**	**37**	2.97×10^4	585
meso-**56**	None		416
meso-**56**	**37**	9.88×10^3	589

complex with geometry **42** because the cyclohexane barrier is too remote from the methyl group of the guest to exert steric repulsion. On the contrary, in the (*R,R*)(*R,R*)-**23**–(*S*)-**29** complex with geometry **41**, steric repulsion between the methyl group and the cyclohexane barrier reduced the strength of the fourth hydrogen bond, thus reducing the stability of this complex.

The geometries **43** and **44** ($R=CH_3$) reasonably interpret the fact that (*S,S*)(*S,S*)-**23** displayed better complementarity to (*S*)-**30** than (*R,R*)(*R,R*)-**23**. It is understandable from geometries **43** and **44** ($R=CH(CH_3)_2$) that (*S,S*)(*S,S*)-**23** fitted (*S*)-**31** better than did (*R,R*)(*R,R*)-**23**, and the relatively small K_a values for complexes with (*S*)-**31** are interpreted in terms of serious steric repulsion between the phenyl barrier and the isopropyl group of large steric requirement.

As expected, the enantiomer selectivity of **24** towards chiral amines except (*S*)-**31** was the reverse of that of **23**. The conformations of diastereoisomeric complexes of **24** with a chiral amine are shown in the general geometries **45** and **46**; the former is more stable. It is rationalized from these geometries that the combinations (*R,R*)(*R,R*)-**24**–(*S*)-ethylamines **33** and **34** led to the more stable complexes whose geometries match with **45** ((*S*)-**33**, $L=C_6H_5$, $M=CH_3$ $S=H$; (*S*)-**34**, $L=1\text{-}C_{10}H_7$, $M=CH_3$ $S=H$). The result that (*R,R*)(*R,R*)-**24** gave the more stable complexes with (*S*)-ethanolamines **29** and **30** than (*S,S*)(*S,S*)-**24** are reasonably interpreted in terms of the geometries **47** and **48** ((*S*)-**29**, $R=H$, $R'=CH_3$; (*S*)-**30**, $R=CH_3$, $R'=H$) because of better complementarity in **47**.

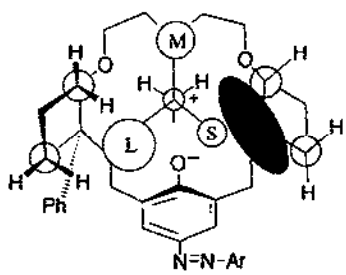

45 [(*R,R*)(*R,R*)-**24**: chiral amine]

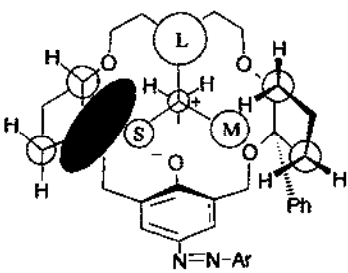

46 [(*S,S*)(*S,S*)-**24**: chiral amine]

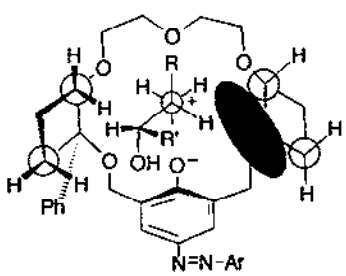

47 [(*R,R*)(*R,R*)-**24**:(*S*)-ethanolamine]

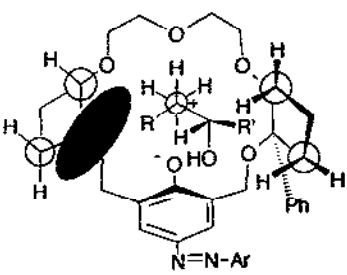

48 [(*S,S*)(*S,S*)-**24**:(*S*)-ethanolamine]

The results mentioned in this section demonstrate that (1) the 1,3-xylyl subunit of **23** and **24** reduced the conformational flexibility of the binding cavity, and thus the cyclohexane moiety functions as a second steric barrier in addition to the phenyl barrier, (2) the alteration in the position of the binding site, that is the phenol moiety, results in reversal of the enantiomer selectivity, and (3) the reduced cavity of **23** and **24** possessing phenyl and the cyclohexane barriers resulted in a reduction in the binding ability toward an amine having a large substituent.

4. Enantiomer recognition of the azophenolic crown ether 28 incorporating *cis*-cyclohexane-1,2-diol as a chiral barrier

The preparation of achiral crown ethers incorporating *cis*-cyclohexane-1,2-diol has been described [15], but no optically active crown ether has been prepared using this diol as a building block. Removal of the phenyl barriers from (*R*,*R*)(*R*,*R*)-**23** and (*R*,*R*)(*R*,*R*)-**24** results formally in (*R*,*S*)(*R*,*S*)-**28** having the cyclohexane moiety as a chiral barrier, which was actually prepared from (1*S*,2*R*)-(−)-**9** via (−)-**27**. The calculated conformation of (*R*,*S*)(*R*,*S*)-**28** (Fig. 3) shows that it possesses a wider binding space than (*R*,*R*)(*R*,*R*)-**23** or (*R*,*R*)(*R*,*R*)-**24** and is expected to exhibit a somewhat larger K_a value for the complex with **31**.

The observation that the combinations (*S*,*R*)(*S*,*R*)-**28**–(*S*)-ethyl amine derivatives (*S*)-**33** and (*S*)-**34** led to stable complexes is understandable from the geometries **49** and **50** which are illustrated for complexes (*R*,*S*)(*R*,*S*)-**28**–chiral amine and (*S*,*R*)(*S*,*R*)-**28**–chiral amine respectively.

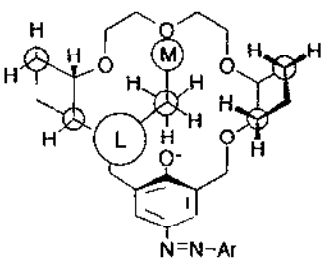

49 [(*R*,*S*)(*R*,*S*)-**28**: chiral amine]

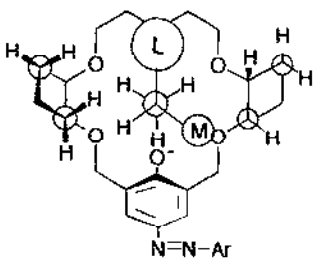

50 [(*S*,*R*)(*S*,*R*)-**28**: chiral amine]

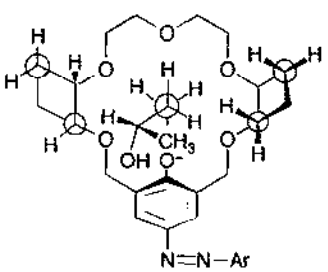

51 [(*R*,*S*)(*R*,*S*)-**28**:(*S*)-**29**]

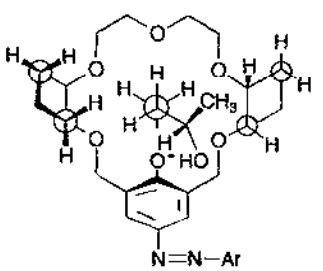

52 [(*S*,*R*)(*S*,*R*)-**28**:(*S*)-**29**]

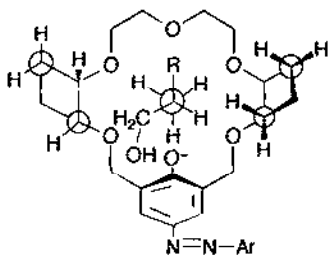

53 [(*R,S*)(*R,S*)-**28**:(*S*)-2-substituted 2-aminoethanol]

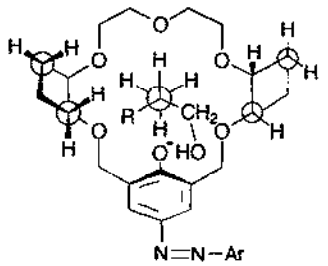

54 [(*S,R*)(*S,R*)-**28**:(*S*)-2-substituted 2-aminoethanol]

The geometry **50** ((*S*)-**33**, L = C_6H_5, M = CH_3; (*S*)-**34**, L = 1-$C_{10}H_7$, M = CH_3), where the group L is placed at the least hindered area over the diethylene glycol bridge and the most hindered area near the cyclohexane barrier is occupied by the hydrogen atom of the amine, reasonably interprets the better complementarity of (*S,R*)(*S,R*)-**28** to (*S*)-ethyl amine derivatives than that of (*R,S*)(*R,S*)-**28**.

Differences in steric repulsion between diastereoisomeric complexes with geometries **51** and **52** are not appreciable, resulting in low enantiomer selectivity of **28** toward (*S*)-**29**.

On the contrary, as expected, the removal of the bulky phenyl barriers enhanced the binding ability of **28** toward (*S*)-**31** and well-defined enantiomer selectivity was observed. It is understandable from geometries **53** and **54** that (*R,S*)(*R,S*)-**28** displayed better complementarity to the (*S*)-guests than (*S,R*)(*S,R*)-**28**, because of the steric repulsion between the cyclohexane barrier and the substituent R destabilizing the (*S,R*)(*S,R*)-**28**–(*S*)-guest complexes with geometry **54** ((*S*)-**30**, R = CH_3; (*S*)-**31**, R = $CH(CH_3)_2$; (*S*)-**32**, R = C_6H_5).

The results described in this section demonstrate that (1) the *cis*-cyclohexane-1,2-diol moiety served as an effective chiral barrier in complexation with 2-aminoethanols and ethylamines of the type $LMSC^*NH_2$, but not in complexation with 1-substituted 2-aminoethanol ($LMSC^*CH_2NH_2$) and (2) removal of the bulky

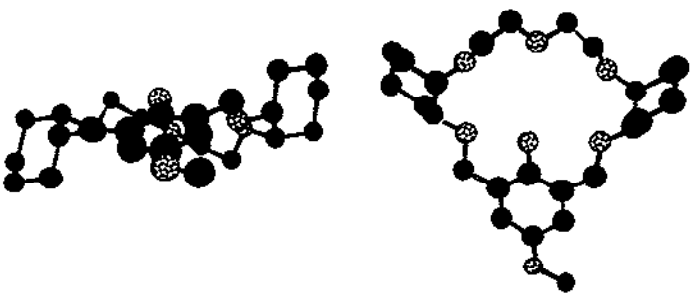

(*R,S*)(*R,S*)-**28**

Fig. 3. Structures of the calculated conformation of (*R,S*)(*R,S*)-28.

barrier enhanced the stability of complex with guests **31**, **33** and **34** possessing a bulky substituent.

5. Diastereotopic face selectivity of *meso*-crown ethers 55 and 56 in complexation with achiral amines

Complexation of alkylammonium cations with chiral crown ethers having diastereotopic faces has been described [16]. However, as far as we know, there has been no report of diastereotopic face selectivity in complexation of alkylamine by the diastereotopic faces of a *meso*-crown ether such as **55** and **56**. The plane of symmetry of **55** and **56** which were prepared from (±)-**6** is perpendicular to the face of the polyether ring and thus they can bind neutral amines to each diastereotopic faces to form diastereoisomeric α and/or β complexes.

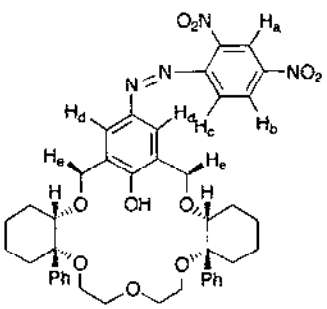

meso-**55**

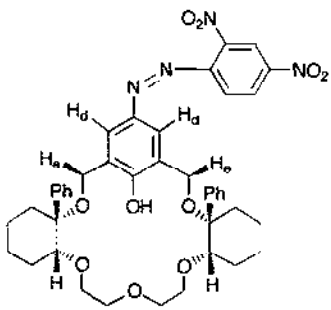

meso-**56**

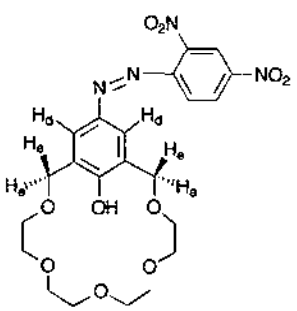

57

The low temperature ^{1}H nuclear magnetic resonance (NMR) spectrum of **55** displaying well-separated signals due to H_a, H_b, H_c, H_d and H_e with unequal intensity suggested that **55** exists in two conformations **58** and **59** where the phenol moiety tilts out of the polyether plane [13] and the diastereoisomeric structures **60** and **61** are illustrated for the β complex and the α complex respectively.

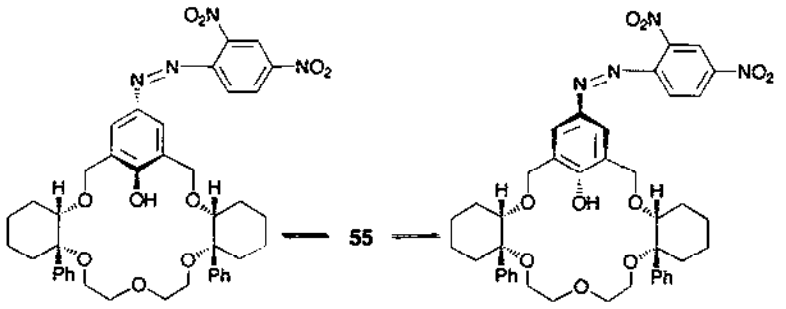

58 55 59

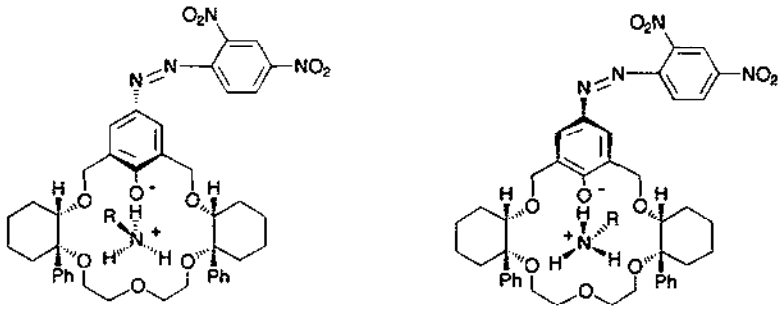

60 61

Diastereotopic face selectivities in complexation of **55** and **56** with achiral amines were examined using temperature-dependent ^{1}H NMR. The spectra indicated that both **55** and **56** bound **35** to form the corresponding α and β complexes in unequal amounts but the spectroscopic data could not indicate clearly which diastereoisomer of the complexes was preferentially formed.

The complexation behaviours of **55** and **56** with **37** were markedly different from those with **35**. When less than one equivalent of **37** was added to **55**, ^{1}H NMR of the mixture revealed two sets of signals with unequal intensities and the signals with low intensity were identified as those of the host. The spectrum of the mixture of **55** with excess of **37** displaying only one set of signals for the complex even at low temperature demonstrated that the host was quantitatively converted into one of the diastereoisomeric complexes.

Next, the prediction of which diastereoisomeric complex of **55** and **37** was exclusively formed is made on the basis of ^{1}H NMR and examination the CPK molecular model of the complex. In the spectrum of the **55**–**37** complex, signals for H_d and H_e were shifted upfield by ca. 0.95 and ca. 1.35 ppm compared with the corresponding chemical shifts in the spectrum of **55**. The upfield shifts observed showed that two phenyl substituents were oriented over these protons in the α complex **63**; that is, complexation occurred at the α face of **55**. CPK molecular models of the complexes show that H_d and H_e are shielded by phenyl barriers in **63** but not in the β complex **62**. The high α face selectivity in complexation is interpreted on the basis of CPK

molecular models suggesting that two cyclohexane residues are brought close together on the α face of **62**, and so steric repulsions between these residues and between the guest and phenyl barriers made **62** less stable than **63**.

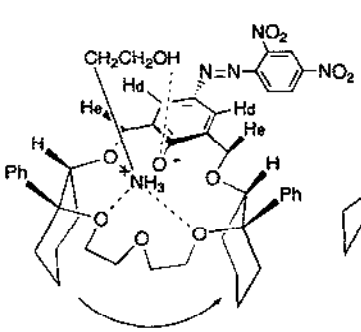

62 [*meso*-**55**:**37**]

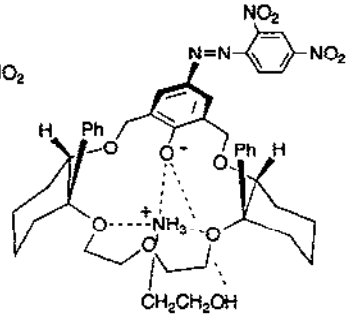

63 [*meso*-**55**:**37**]

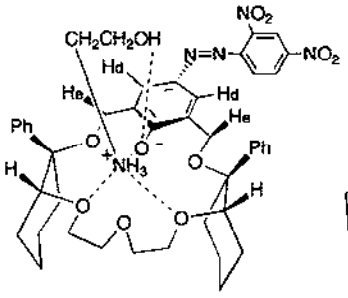

64 [*meso*-**56**:**37**]

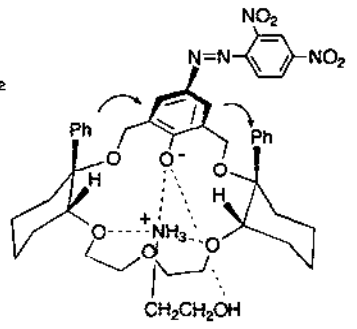

65 [*meso*-**56**:**37**]

Similarly, the ^{1}H NMR spectrum of the mixture of **56** with **37** showed that the amine was attached to one of the faces of **56** to form exclusively the β complex **64** because no upfield shift of the signals for H_d and H_e was observed in its spectrum. The CPK molecular model of the α complex **65** indicates that H_d and H_e should be oriented within the shielding zones of phenyl groups. In contrast to the α face selectivity in complexation of **55** with **37**, the amine was attached preferentially to the β face of **56** despite two bulky phenyl barriers on the β face. The observation is rationalized on CPK molecular model examination suggesting that two phenyl barriers and the phenol moiety are brought close together on the β face of **65** and their large steric repulsion overcomes the repulsion between the phenyl barriers and the guest in **64** resulting in high β face selectivity. The relatively small K_a value for the β complex **56**–**37** compared with that for the α complex **55**–**37** is assumed to be due to large steric repulsion between the cyclohexane moieties on the α face and between the phenyl barriers and the guest on the β face in **64**.

The results demonstrated that (1) the diastereotopic face selectivity varied with the guest, (2) the alteration in the position of the phenyl steric barriers with respect

to the phenol moiety resulted in reversal of the diastereotopic face selectivity, and (3) steric repulsions between the groups of the host played a crucial role in determining the diastereotopic face selectivity.

The observed singlet signal for H_d in **63** and **64** at 35 °C showed that the two H_d protons were homotopic because of free rotation about the C–N bond of the azophenolic residue at this temperature. However, this signal separated into two singlets of equal intensity at −50 °C suggesting that the complexes **63** and **64** lost their plane of symmetry at low temperature. The same separation of signals for H_d and H_e was observed in ^1H NMR spectrum of the **57–37** complex. We assume that restricted rotation about the C–N bond of **66** resulting from a contribution of a quinoid structure such as **67** made these protons heterotopic (H_d and $H_{d'}$; H_e and $H_{e'}$) at low temperature.

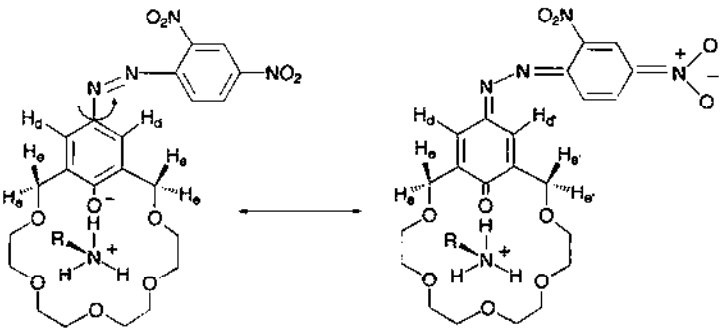

An earlier paper [13] showed using X-ray crystallographic analysis of the complex of **18** ($X = NO_2$) with an ammonium salt that there is a significant contribution from a quinoid form with the formal negative charge delocalized into the nitrophenyl ring.

Previous reports [6,17] on the enantiorecognitive coloration of azophenolic crown ethers have explained the observed blue shift in the UV–visible spectrum, the difference in transition energy between diastereoisomeric complexes with chiral amines, in terms of better host–guest complementarity as indicated by CPK molecular models of the complex. The elucidation of this problem is essential for the development of a host–guest colour indicator, hence our study to clarify a correlation between enantiorecognitive coloration and host–guest complementarity, judged experimentally by association constants, will be continued.

References

[1] C.J. Pedersen, J. Am. Chem. Soc., 89 (1967) 2495. C.J. Pedersen, J. Am. Chem. Soc., 89 (1967) 7017.

[2] R.M. Izatt and J.J. Christensen (Eds.) Synthetic Multidentate Macrocyclic Compounds, Academic Press, New York, 1978, p. 1. R.M. Izatt and J.J. Christensen (Eds.), Progress in Macrocyclic Chemistry, Vol. 1, Wiley, New York, 1979, p. 1. J.F. Stoddart, Chem. Soc. Rev., 8 (1979) 85. J.F. Stoddart, Synthetic chiral receptor molecules from natural products, in R.M. Izatt and

J.J. Christensen (Eds.) Progress in Macrocyclic Chemistry, Vol. 2, Wiley–Interscience, New York, 1981, p. 173. G.W. Gokel and S.H. Korzeniowski, Macrocyclic Polyether Syntheses, Springer, New York, 1982. P.G. Potvin and J.-M. Lehn, Design of cation and anion receptors, catalysts and carriers, in R.M. Izatt and J.J. Christensen (Eds.), Synthesis of Macrocycles: the Design of Selective Complexing Agents, Wiley–Interscience, New York, 1987, p. 167. J.F. Stoddart, Chiral crown ethers, in Topics in Stereochemistry, Vol. 17, New York, 1988, p. 207. R.M. Izatt, K. Pawlak, J.S. Bradshaw and R.L. Bruening, Chem. Rev., 91 (1991) 1721, and references cited therein.

[3] E.B. Kyba, M.G. Siegel, L.R. Sousa, G.D.Y. Sogah and D.J. Cram, J. Am. Chem. Soc., 95 (1973) 2961. E.P. Kyba, K. Koga, L.R. Sousa, M.G. Siegel and D.J. Cram, J. Am. Chem. Soc., 95 (1973) 2692. R.C. Helgeson, J.M. Timko, P. Moreau, S.C. Peacock, J.M. Mayer and D.J. Cram, J. Am. Chem. Soc., 96 (1974) 2762. L.R. Sousa, D.H. Hoffman, L. Kaplan and D.J. Cram, J. Am. Chem. Soc., 96 (1974) 7100. D.J. Cram, R.C. Helgeson, L.R. Sousa, J.M. Timko, M. Newcomb, P. Moreau, F. de Jone, G.W. Gokel, D.H. Hoffman, L.A. Domeier, S.C. Peacock, K. Madan and L. Kaplan, Pure Appl. Chem., 43 (1975) 327. E.P. Kyba, J.M. Timko, L.J. Kaplan, F. de Jong, G.W. Gokel and D.J. Cram, Pure Appl. Chem., 100 (1978), 4555. R.D.Y. Sogah and D.J. Cram, Pure Appl. Chem., 101 (1979) 3035. D.J. Cram, Angew. Chem., Int. Edn. Engl., 27 (1988) 1009, and references cited therein.

[4] K. Naemura, I. Ebashi and M. Nakazaki, Bull. Chem. Soc. Jpn., 58 (1985) 767. K. Naemura and R. Fukunaga, Chem. Lett., (1985) 1651. K. Naemura, R. Fukunaga and M. Yamanaka, J. Chem. Soc., Chem. Commun., (1985) 1560. K. Naemura, I. Ebashi, A. Matsuda and H. Chikamatsu, J. Chem. Soc., Chem. Commun., (1986) 666. K. Naemura, K. Komatsu, K. Adachi and H. Chikamatsu, J. Chem. Soc., Chem. Commun., (1986) 1675. K. Naemura, T. Matsumura, M. Komatsu, Y. Hirose and H. Chikamatsu, J. Chem. Soc., Chem. Commun., (1988) 239. K. Naemura, R. Fukunaga, M. Komatsu, M. Yamanaka and H. Chikamatsu, Bull. Chem. Soc. Jpn., 62 (1989) 83. K. Naemura, T. Matsumura, M. Komatsu, Y. Hirose and H. Chikamatsu, Bull. Chem. Soc. Jpn., 62 (1989) 3523. K. Naemura and M. Ueno, Bull. Chem. Soc. Jpn., 63 (1990) 3695.

[5] K. Naemura, H. Miyabe and Y. Shingai, J. Chem. Soc., Perkin Trans. 1, (1991) 957. K. Naemura, H. Miyabe, Y. Shingai and Y. Tobe, J. Chem. Soc., Perkin Trans. 1, (1993) 1073.

[6] T. Kaneda, K. Hirose and S. Misumi, J. Am. Chem. Soc., 111 (1989) 742.

[7] K. Naemura, K. Ueno, S. Takeuchi, Y. Tobe, T. Kaneda and Y. Sakata, J. Am. Chem. Soc., 115 (1993) 8475.

[8] K. Naemura, S. Takeuchi, K. Hirose, Y. Tobe, T. Kaneda and Y. Sakata, J. Chem. Soc., Perkin Trans. 1, (1995) 213.

[9] K. Naemura, S. Takeuchi, M. Asada, K. Hirose, Y. Tobe, T. Kaneda and Y. Sakata, J. Chem. Soc., Chem. Commun., (1994) 711.

[10] M.P. Schneider, Enzymes as Catalysts in Organic Synthesis, Reidel, Dordrecht, 1986. D.H.G. Crout and M. Christen, in R. Scheffold (Ed.) Modern Synthetic Method, Vol. 5, Springer, Berlin, 1989, p. 1. C.-H. Wong, Science, 244 (1989) 1145. E.J. Toone, E.S. Simon, M.B. Bednarski and G.M. Whitesides, Tetrahedron, 45 (1989) 5365. L.-M. Zhu and M.C. Tedford, Tetrahedron, 46 (1990) 6587. H.G. Davies, R.H. Green, D.R. Kelly and S.M. Roberts, Biotransformations in Preparative Organic Chemistry, Academic Press, London, 1990.

[11] A.M. Klibanov and B. Cambou, J. Am. Chem. Soc., 106 (1984) 2687. C.-S. Chen, S.-H. Wu, G. Girdaukas and C.J. Sih, J. Am. Chem. Soc., 109 (1987) 2812. G. Gil, E. Ferre, M. Moeou, J.L. Petit and C. Triantaphylides, Tetrahedron Lett., 28 (1987) 1647. Z.W. Guo and C.J. Sih, J. Am. Chem. Soc., 110 (1988) 1999, and references cited therein.

[12] M. Newcomb, J.L. Toner, R.C. Helgeson and D.J. Cram, J. Am. Chem. Soc., 101 (1979) 4941.

[13] C.H. Browne, G. Ferguson, M.A. McKervy, D.L. Mulholland, T. O'Connor and M. Parvez, J. Am. Chem. Soc., 107 (1985) 2703.

[14] H.A. Benesi and J.H. Hildebrand, J. Am. Chem. Soc., 71 (1949) 2703.

[15] C.J. Pedersen, J. Am. Chem. Soc., 89 (1967) 7017. C.J. Pedersen, J. Am. Chem. Soc., 92 (1970) 391. R.M. Izatt, B.L. Haymore, J.S. Bradshow and J.J. Christensen, J. Inorg. Chem., 14 (1975) 3132.

[16] D.A. Laidler and J.F. Stoddart, J. Chem. Soc., Chem. Commun., (1977) 481. R.B. Pettman and J.F. Stoddart, Tetradhedron Lett., (1979) 457. R.B. Pettman and J.F. Stoddart, Tetrahedron Lett., (1979) 461. D.A. Laidler, J.F. Stoddart and J.B. Wolstenholme, Tetrahedron Lett., (1979) 465. S.E. Fuller, B.E. Mann and J.F. Stoddart, J. Chem. Soc., Chem. Commun., (1982) 1096.

[17] K. Yamamoto, K. Isoue, Y. Sakata and T. Kaneda, J. Chem. Soc., Chem. Commun., (1992) 791.